



## Design and seismic performance of multi-storey frames with intentionally eccentric braces

Andrés González Ureña<sup>1</sup>, Robert Tremblay<sup>2</sup>, Colin Rogers<sup>3</sup>

<sup>1</sup> Ph.D. student, Department of Civil Engineering and Applied Mechanics, McGill University - Montréal, QC, Canada.

<sup>2</sup> Professor, Department of Civil, Geological and Mining Engineering, Polytechnique Montréal - Montréal, QC, Canada.

<sup>3</sup> Professor, Department of Civil Engineering and Applied Mechanics, McGill University - Montréal, QC, Canada.

### ABSTRACT

This paper presents a study on the seismic response of steel braced frames with bracing members built with intentional eccentricity. Being subject to bending moment in addition to axial force under seismic action, braces with intentional eccentricity (BIEs) inherently possess lower stiffness than conventional braces and are characterised by a pseudo-trilinear force-displacement behaviour in tension and a smooth flexural response in compression devoid of sharp peaks due to buckling. Moreover, their pre- and post-yielding stiffness can be adjusted by varying the eccentricity, allowing for a better control of the structure's dynamic response. A preliminary design methodology, based on the Direct Displacement-Based Design approach, is proposed and applied to the earthquake-resistant design of five- and ten-storey buildings located in Vancouver, BC, Canada. The seismic performance of the buildings is assessed through dynamic non-linear response-history analysis. The proposed system is found to provide an acceptable response complying with NBCC 2015 limiting drift ratios and capacity-based design philosophy, while proving to be economically advantageous in comparison to buildings designed with conventional braced frames.

Keywords: steel braces, intentional eccentricity, earthquake-resistant design, displacement-based design, non-linear response-history analysis.

### INTRODUCTION

Concentrically braced steel frames (CBFs) constitute a common selection for the seismic-force-resisting system of low and mid-rise buildings, in which they are intended to provide lateral stiffness and resistance and dissipate energy inelastically through cycles of yielding in tension and buckling in compression, allowing for up to a moderately ductile response. Hollow structural sections (HSSs) are frequently used for the bracing members in these systems as they provide high resistance in compression in relation to their gross area, possess high torsional stiffness and are aesthetically convenient. However, the range of HSSs complying with modern design codes, such as the CSA S16 Standard [1], is restricted due to stringent limitations on global and local (cross-section) slenderness that intend to ensure minimum ductility and energy dissipation while reducing the probability of brace fracture. A lower limit of 70 is set for the global slenderness ratio,  $KL/r$ , of HSS bracing members as it has been shown that HSS braces with lower slenderness are prone to fracturing prematurely at the plastic hinge region [2, 3]. Similarly, the width-to-thickness,  $b_e/t$ , ratio is circumscribed by an upper limit that depends on the global slenderness to also prevent low-cycle fatigue fracture triggered by local buckling [2]. Another significant drawback of CBFs is their invariably high elastic stiffness, as it constrains the structure to low fundamental periods of vibration and thus to high acceleration and force demands. Moreover, the intrinsic overstrength that arises from the compression resistance controlling the sizing of the bracing members, results in higher design forces than for other systems, requiring the use of heavier capacity protected connections, beams and columns, and imposing greater force demands on the foundation which can be costly to accommodate.

To address these shortcomings of CBFs, intentionally offsetting the axis of otherwise conventional steel braces with respect to their working point has been proposed in [4] as a means to improve certain characteristics of their force vs. deformation hysteretic response. Being subject to bending moment in addition to axial force under seismic action, braces with intentional eccentricity (BIEs) inherently possess lower stiffness than conventional buckling braces (CBBs) and are characterised by a pseudo-trilinear force-displacement behaviour in tension and a smooth flexural response in compression devoid of sharp peaks due to buckling. Moreover, their pre- and post-yielding stiffness can be adjusted by varying the eccentricity, allowing for a better control of the structure's dynamic response to ground motion excitation. In [4], cyclic load tests were performed on five half-scale specimens of BIEs with two eccentricity values and one conventional concentric brace, all made from the same circular HSS. Their results are consistent with the behaviour described above, and indicate that in comparison with CBBs, local buckling and fracture occur in BIEs at significantly higher drift ratios due to strain demands being more evenly distributed

along the brace length. However, their study has not been continued to investigate the application of these braces in buildings nor to address their implementation in a global design approach.

In the present paper, a precursory investigation on the use of frames with intentionally eccentric braces (FIEBs) for the seismic-force-resisting system (SFRS) of multi-storey buildings is presented as an early step intending to shed light on whether FIEBs may constitute a competent SFRS, consistent with modern earthquake-resistant design philosophy. Under this scope, a preliminary design methodology, based on the Direct Displacement-Based Design approach (DDBD) [6] is proposed and applied to the design of five- and ten-storey example buildings located in Vancouver, British Columbia, Canada. The performance of the buildings is then assessed through dynamic non-linear response-history analysis (NLRHA).

## FORCE-DEFORMATION BEHAVIOUR OF BIEs

### Monotonic response in tension and compression

Figure 1.a presents schematically the main components of a BIE. The eccentricity,  $e$ , is defined as the parallel offset between the axis of the bracing member and the line linking the frame working points. The eccentricity is introduced by means of plate assemblies, which will be hereon referred to as *eccentering* assemblies, designed to transfer rigidly the axial loads between the working points and the bracing member. The kinematical behaviour of BIEs as described in [4], and as assumed in the present research, relies on the assumption that the connections at the ends of the *eccentering* assemblies behave as pins. In practice, this behaviour can be easily achieved by using knife plate to gusset plate end connection to produce in-plane bending of the BIEs, as illustrated in Figure 1.b. This configuration was adopted in this research because of its simplicity and cost-effectiveness. It also prevents storey drifts from imposing in-plane bending moments on the BIEs in addition to those arising from their eccentricity, leading to a simpler and predictable brace hysteretic behaviour.

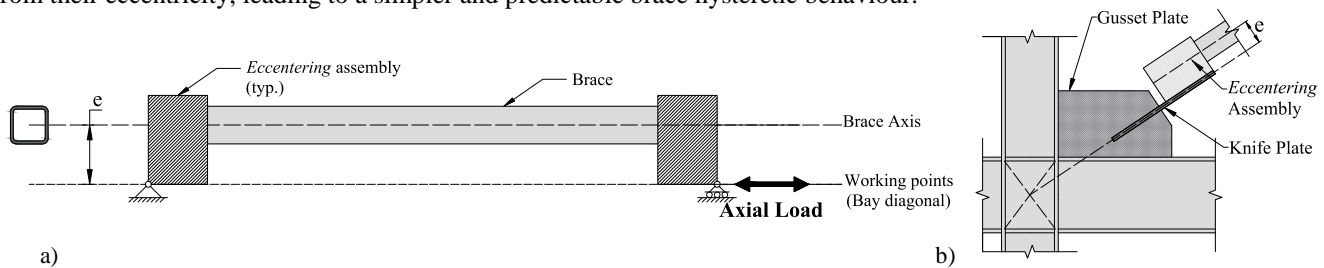


Figure 1. a) Schematic drawing of a BIE and its components; b) Schematic drawing of knife plate to gusset plate connection

Due to the eccentric loading, in addition to an axial force, the BIE is subjected to a bending moment with initial magnitude equal to the product of the axial force and the eccentricity. Figure 2 shows the idealised general monotonic behaviour in tension and in compression of BIEs, compared to that of CBBs. Under tensile load, the BIE responds by bending toward the working point axis as it elongates. Since the moment arm across the brace length decreases as loading progresses, the effective stiffness increases with the axial deformation until the outermost fiber in tension attains the yielding stress,  $F_Y$ . The corresponding point on the curve,  $T_Y - \Delta_Y$ , can be designated as the “first yield” point, as it marks a significant discontinuity on the force-deformation response. As loading is continued beyond this point, plasticity progresses through the cross-section and the BIE responds with a lower effective stiffness that, however, increases as the moment arm keeps decreasing. The maximum tensile force developed by the BIE,  $T_U$ , is attained when the complete cross-section yields; this occurs when the eccentricity has reduced to zero at the mid-length region, which is then under pure tension. Nearing this stage, plastic hinges may develop where the brace ends meet the *eccentering* assemblies as the rotation demand there is at its peak. Compared to a CBB, the BIE attains its maximum capacity at significantly larger axial deformation levels depending on the eccentricity.

The force-deformation backbone curve of BIEs in tension can be idealised with a tri-linear model, as proposed in [4]: an initial, or elastic, portion with initial stiffness,  $K_i$ , until attaining the “first-yield” point,  $T_Y$ , followed by a post-first-yield portion with secondary stiffness,  $K_s$ , limited by the ultimate yield point,  $T_U$ , and a final portion where the section is fully yielded until fracture. Equations for  $T_Y$ ,  $K_i$  and  $K_s$  were proposed in [4]. However, in this present research the preliminary results obtained from numerical finite element models suggest that they are appropriate only for a limited range of sections and  $KL/r$  ratios, as they neglect second-order effects before “first yielding” and the influence of the *eccentering* assembly’s length and stiffness.

When compressive load is applied, the BIE bends away from the working points axis and the increment in the brace deflection entails a progressive reduction in the stiffness as the effective moment arm at the brace mid-length increases. The maximum force developed in compression,  $C'$ , can be approximated by the critical load of column subjected to eccentric axial load as proposed in [4]. In contrast with CBBs, the maximum force in compression in BIEs does not manifest as a sharp peak in the force-deformation curve. Instead, the response transitions smoothly from elastic behaviour to post-buckling behaviour, with the residual force in the BIE tending toward that of the CBB. As such, the backbone curve of BIE response in compression can

be idealised with an elastic-perfectly plastic model, with initial stiffness  $K_i$  and maximum force  $C'$  (Fig. 2). As loading progresses further, a plastic hinge develops at the brace mid-length where all strain demand concentrates.

The influence of the eccentricity value on  $T_y$ ,  $K_i$  and  $K_s$  can be observed in Figure 3, which was obtained from analyses carried with the OpenSees platform [5] on fiber models of monotonically loaded BIEs of a G40.21-350W HSS 127×127×8 member, with a hinge-to-hinge length of 5470 mm and rigid *eccentering* assemblies 300 mm long. These dimensions are consistent with those of a brace used in a 6 m wide bay with 4 m storey height. The hinge regions were detailed as a 44 mm long clearance on the 22 mm thick by 300 mm wide knife plate to allow for unrestrained plastic rotation. It was verified through additional analyses that this detail produced a response very close to that of a BIE with pinned connections. In the figure, it can be observed how, by varying the magnitude of the intentional eccentricity, all other parameters being fixed, the primary and secondary stiffness can be adjusted. Extrapolated to the design of a full braced frame, this characteristic of BIEs would presumably allow for a better control of the structure's dynamic response to ground motion excitation.

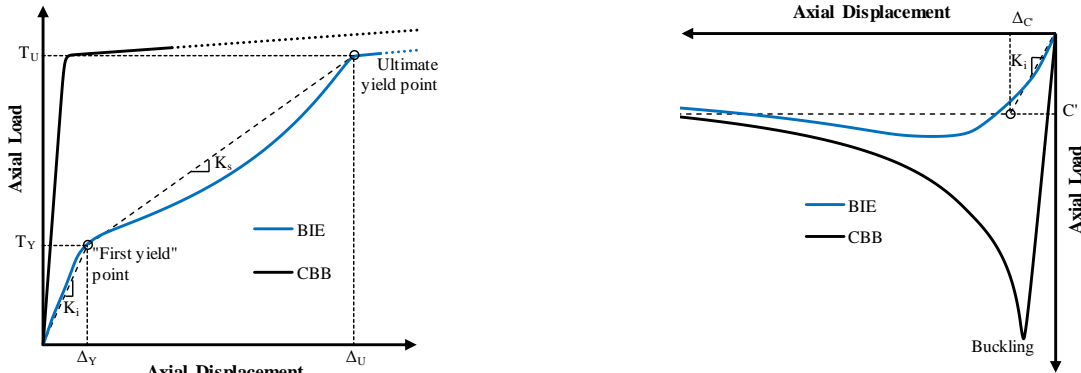


Figure 2. Compared BIE and CBB idealised monotonic behaviour: tension (left) and compression (right) (not to scale)

### Response of BIEs under cyclic loading

In Figure 4, axial force vs. lateral drift hysteretic plots of an HSS 178×178×10 BIE with an eccentricity of 200 mm and a CBB of the same section, obtained from OpenSees analyses, are presented. The BIE dimensions and components were again defined assuming a braced bay 6 m by 4 m, and a loading protocol with symmetrical cycles of increasing equivalent storey drift amplitude of 0.1, 0.25, 0.75, 1.0, 1.5, 2 and 3 % was followed. It can be noted how the BIE exhibits a significant secondary, or post-yield, stiffness in tension with the maximum load increasing at each cycle, while in compression the maximum load is stabilized at the post-buckling force level. The physical tests in [4] also showed that in comparison with CBBs, the development of local buckling in BIEs is delayed to higher deformation demands, thus reducing the probability of premature fracture. The generalisation of these findings to square HSS BIEs with different  $KL/r$  and  $b_{el}/t$  ratios, made from North-American steel is expected to be confirmed through a detailed finite element analysis and a full-scale physical testing program that are subsequent phases of this research.

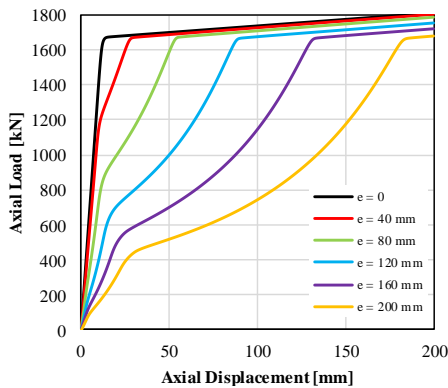


Figure 3. Influence of eccentricity in tension force-displacement behaviour for a 127×127×8 HSS with  $L=5470$  mm

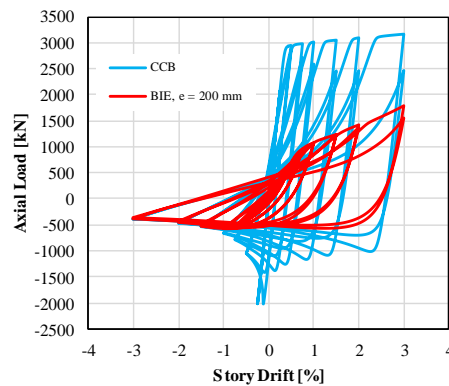


Figure 4. Axial force vs. lateral drift for a 178×178×10 HSS BIE and CBB under cyclic load

### PRELIMINARY DESIGN METHODOLOGY FOR FIEBs

Due to their particular force-deformation behaviour in tension, the conventional force-based procedure used with Type MD-, LD- and CC- CBF systems [1, 7] is not suitable for BIEs. For CBBs, the force-deformation behaviour is idealised as elastic-

perfectly plastic. As such, the braces can be dimensioned by equating their yield strength to the seismic demand resulting from an elastic analysis, in which the force level is reduced by the  $R_d$  and  $R_o$  factors to account for ductile response and overstrength. In the case of BIEs, the maximum capacity in tension is attained at deformation levels that depend on the specified eccentricity and that might be too large to be compatible with the maximum allowable storey drift ratios used in design (2.5 % for buildings of the normal importance category in [7]).

Furthermore, their secondary stiffness is significant and varies with the section properties, the member slenderness and the eccentricity, making both an elastic-perfectly plastic idealisation and the use of the ductility reduction factor,  $R_d$ , unfitting. Given these considerations, the development of a displacement-based design procedure, consistent with the DDBD method described by Priestley et al. [6], appears as a rational choice adaptable to the BIEs force-deformation curve. The appropriateness of the DDBD approach for the design of CBFs has been demonstrated in past research [8, 9] and the results presented in this paper can be considered as a preliminary verification of its applicability to FIEBs. In the following sections, the steps of the preliminary design methodology used in this research are briefly described. For general information on DDBD refer to [6].

### 1. Select target storey drift and displacement vector and calculate associated equivalent mass and equivalent displacement

The displacement vector used in DDBD generally corresponds to the inelastic first mode shape specific to the structural system and the height of the building. In the case of FIEBs, no information on this is yet available as this is the first research that investigates their use as a SFRS. The formal calibration of this parameter will require extensive study that could be performed at a later stage after the potential of the new system has been demonstrated. It is also important to note that this displacement vector in DDBD methods is a design assumption that does not necessarily reflect the maximum anticipated seismic displacements, since it does not incorporate the effects of higher modes nor the influence of the reversing nature of earthquake demands. In the present research, the inelastic first mode shape proposed in [6] for moment frames, given by Equation (1), is used. This approximation has been used in DDBD procedures for CBFs in past research, such as [8] and [10], to satisfactory success. In (1),  $n$  is the number of storeys,  $H_i$  and  $H_n$  are the elevations of the  $i^{\text{th}}$  and top storeys and  $\delta_i$  is the normalised lateral displacement of the  $i^{\text{th}}$  storey.

$$\begin{aligned} n \leq 4: \quad & \delta_i = \frac{H_i}{H_n} \\ n > 4: \quad & \delta_i = \frac{4}{3} \left( \frac{H_i}{H_n} \right) \left( 1 - \frac{H_i}{4H_n} \right) \end{aligned} \quad (1)$$

The normalised vector obtained with (1) is then scaled so that the lateral design drift of the critical storey corresponds to the selected target storey drift ratio to obtain the storey design displacements,  $d_i$ , which together with the storey masses,  $m_i$ , allow the calculation of the displacement and mass of the equivalent SDOF system at the design level using Equations (2) and (3):

$$\Delta_{eq} = \frac{\sum d_i^2 m_i}{\sum d_i m_i} \quad (2)$$

$$M_{eq} = \frac{\sum d_i m_i}{\Delta_{eq}} \quad (3)$$

### 2. Define equivalent damping ratio and read target period from damped displacement design spectrum

Knowing the target equivalent displacement,  $\Delta_{eq}$ , the target period,  $T_{eq}$ , can be obtained from the damped displacement design spectrum. To do so, the equivalent damping,  $\xi_{eq}$  must first be defined. As for the displacement vector, the formal derivation of equations to predict the equivalent damping ratio at the design level is out of the scope of this preliminary study. Instead, the equivalent damping ratios are estimated, and then their accuracy is verified through iteration. The damped displacement design spectrum is obtained by converting the conventional 5 % damping acceleration,  $S_a$ , design spectra, as given in [7], or the incumbent code, to a displacement,  $S_d$ , spectrum with Equation (4) and scaling it by the damping correction factor,  $R\xi$ , which for the case of this research corresponds to that used in [11] as given by Equation (5).

$$S_d = S_a \frac{T^2}{4\pi^2} \quad (4)$$

$$R\xi = \sqrt{\frac{0.1}{0.05 + \xi_{eq}}} \quad (5)$$

### 3. Calculate target “primary” secant stiffness and corresponding base shear, and obtain equivalent static force vector

Knowing  $T_{eq}$ , the target “primary” secant stiffness,  $K_{eq}$ , is calculated with Equation (6). This stiffness, which is directly associated with the target spectral displacement of the equivalent SDOF system, is labeled “primary” to distinguish it from

“auxiliary” stiffness which the FIEB might require for stability, as explained below. Using  $K_{eq}$ , the equivalent primary base shear,  $V_{eq}$  is obtained from Equation (7) and the corresponding lateral forces are distributed over the height of the building using Equations (8) and (9), with  $F_t$  intending to account for higher mode effects in long period buildings.

$$K_{eq} = 4\pi^2 \frac{M_{eq}}{T_{eq}^2} \quad (6)$$

$$V_{eq} = K_{eq} \Delta_{eq} \quad (7)$$

$$F_{eq,i} = (V_{eq} - F_t) \frac{W_i h_i}{\sum_{i=1}^n W_i h_i} \quad (8)$$

$$F_t = 0.07 T_{eq} < 0.25 V_{eq} \quad (9)$$

(for  $T_{eq} > 0.7$  s)

**4. Select section-eccentricity pairs for each storey, providing capacity equal to the design shear at the design displacement level and complying with regularity and minimum stiffness conditions**

At each storey, the BIEs, which are specified in terms of a section-eccentricity pair (e.g. HSS 178×178×10 – e = 200 mm), are selected such that the storey shear capacity they provide at the target storey displacement  $d_i$  is equal to or slightly exceeds, the design shear. The storey design shear, calculated with Equation (10) is defined as the sum of the equivalent primary storey shear,  $v_{eq,i}$  (from the  $F_{eq,i}$  obtained in step 3) and the notional loads,  $v_{n,i}$ , amplified by the factor  $U_{2,i}$  calculated with Equation (11), in which for each storey  $v_i^*$  is the shear force developed by the section/eccentricity pair at the design displacement.

$$v_{d,i} = U_{2,i} (v_{eq,i} + v_{n,i}) \quad (10)$$

$$U_{2,i} = 1 + \left( \frac{C_{f,i} d_i}{v_i^* h_i} \right) \quad (11)$$

The selection of the BIE section-eccentricity pairs can rely on idealised models of the monotonic behaviour of the BIEs in tension and compression as described in Figure 2, allowing one to estimate the brace force as a function of the storey drift. These can be obtained from numerical analyses under monotonic load performed on models based on design mechanical properties of the material ( $F_Y$ ), replicating the actual dimensions the BIE will have in the braced bent, in particular its hinge to hinge distance and the length of the *eccentering* assemblies, which can be considered as rigid bodies.

To prevent geometric instability, which might be an issue in the case of tall buildings, considering that FIEBs are a significantly more flexible system than CBFs, it is suggested that the  $U_2$  factor be kept less than 1.4 in every storey, as currently specified in [1]. Through a number of evaluations with different  $U_2$  values, the authors have found that this upper limit suffices to reduce the probability of collapse due to geometrical instability. However, further research is required to demonstrate this. Similarly, it was found that, to avoid soft-storey mechanisms and concentrations of shear in particular storeys, compliance with the vertical stiffness regularity condition as defined in [7] is necessary. The BIEs selected at each storey must then, in addition to providing enough shear capacity, develop stiffness at the design displacement level such that these minimum stiffness and regularity criteria are observed.

**5. Design protected members of the FIEB to withstand elastically the probable forces imposed by the action of the BIEs**

Consistent with Capacity-Based Design principles, the non-dissipating components of the FIEBs, i.e. beams, columns, connections and foundations, are treated as protected members and sufficient capacity is provided for them to respond elastically to the forces imposed by the inelastic action of the BIEs. Since the forces developed in the braces depend on the storey drift level, their probable forces are calculated assuming a maximum storey drift level 20 % higher than the target drift level to include a safety margin and to consider the uncertainty on the actual displacement prediction. To consider probable material properties, these amplified brace forces are augmented by  $R_Y$ . Given that in compression the force-displacement behaviour can be approximated with an elastic-perfectly plastic model, no distinction between buckling and post-buckling cases when analysing the forces imposed by the braces on the rest of the structure is needed.

**6. Assess performance of resulting design**

Once the design has been completed, the performance of the building should be assessed through a detailed analysis such as NLRHA to verify the fulfillment of the performance objectives and whether the design assumptions, i.e. target displacement profiles and equivalent damping, are consistent with the actual response of the structure. The structure must also satisfy serviceability and ultimate limit states associated to wind loading.

## PERFORMANCE OF MULTI-STOREY FIEBs

Five- and ten-storey example buildings, based on the same plan configuration shown in Figure 5 (left), and located in Vancouver, BC, were designed as conventional Type MD- and LD-CBFs, as well as FIEBs with square G40.21-350W HSSs for the bracing members using the preliminary displacement-based design procedure described above. A braced frame configuration with pairs of single diagonals acting in opposite directions in adjacent bays was selected (Figure 5, right). In the case of the FIEBs, the connection to the frame is based on a bolted gusset- and knife-plate assembly designed for in-plane bending of the brace (Figure 6). The eccentricity is introduced by two side-plates that link the HSS to the knife plate, which includes a clearance twice its thickness where hinging in flexure is expected to occur.

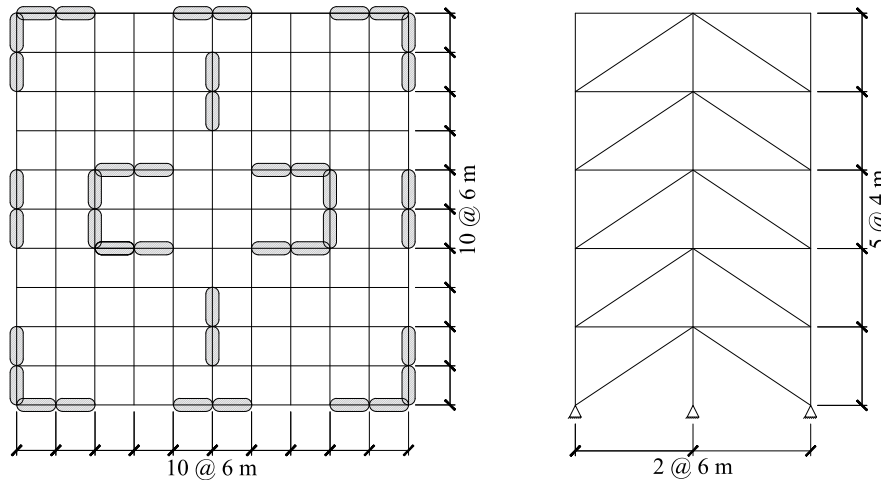


Figure 5. Plan configuration of considered building (left), with highlighted regions indicating location of braced frames and vertical configuration of considered SFRS (right) (5-storey frame shown)

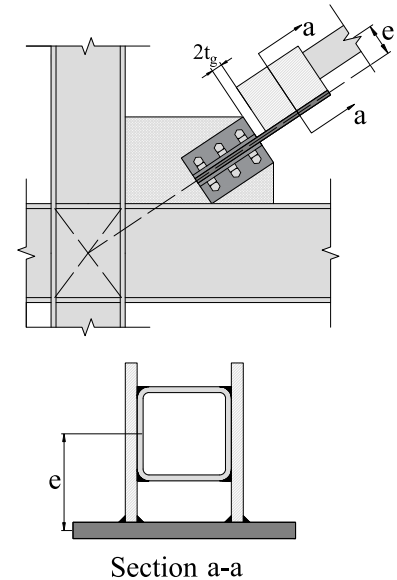


Figure 6. Example of considered BIE to frame joint connection and eccentricity assembly

The five-storey building was designed for a target maximum storey drift of 2.5 %, which coincides with the upper allowable limit for normal importance buildings in [7]. Two versions were designed for the 10-storey building: with 1.5 % and 2.5 % as target maximum storey drift. The performance of the resulting FIEB buildings was assessed through NLRHA of fiber models in OpenSees, using a suite of 5 scaled ground motion records for each of the 3 seismic sources contributing to the seismic hazard in Southwest British Columbia: shallow crustal earthquakes, deep in-slab subduction earthquakes, and large interface subduction events [7, 12]. Only horizontal acceleration was considered.

Figure 7 presents the resulting design for the 10-storey FIEB designed for a target drift of 2.5 %, while Figures 8 to 11 present, for the same building, the maximum storey drifts, the residual storey drifts, the maximum storey shears and the first storey shear vs. drift history when subjected to the acceleration records that produced the highest overall demands on the structure. Note that over the height of the building only two different HSS were specified, while varying the eccentricity. By changing only this parameter, there is a better control on the effective stiffness of each storey and abrupt vertical stiffness discontinuities are avoided. As observed in Figure 8, the performance of the building can be considered acceptable as for the maximum drifts, both the 84<sup>th</sup> percentile and the mean of the five largest values, both calculated from the responses of the 15 records, are smaller than the target 2.5 % limit. This value was exceeded for only one of the interface subduction records, the same one that produced residual drifts over 0.5 % (Figure 9). It can be noted, however, that the design drift profile differs from the average response, which is not surprising, as the latter does not account for higher mode effects nor the load reversing nature of the earthquakes. Regarding the maximum storey shears, Figure 10 shows that the actual storey shears did not surpass in any case the anticipated probable shears, which suggests that the capacity-based design provisions incorporated in the preliminary design procedure had a satisfactory outcome. Finally, from Figure 11 it should be noted that, even for an acceleration record that produced demands significantly larger than those anticipated and significant ratcheting toward one direction, the FIEB showed no strength or stiffness deterioration at the very large drifts that were experienced.

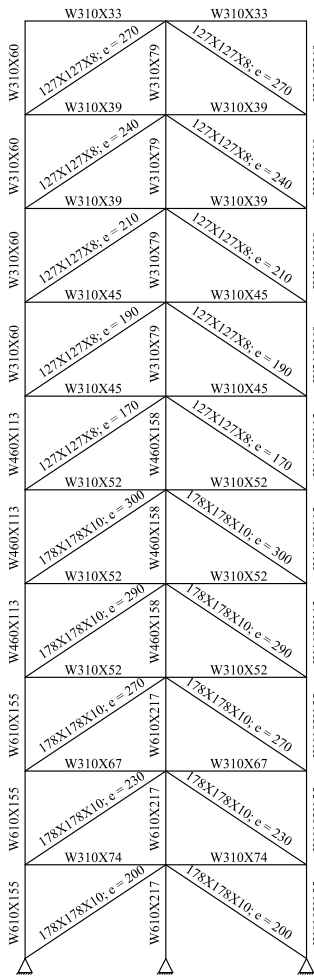


Figure 7. Resulting design for 10-storey FIEB designed with 2.5% target drift

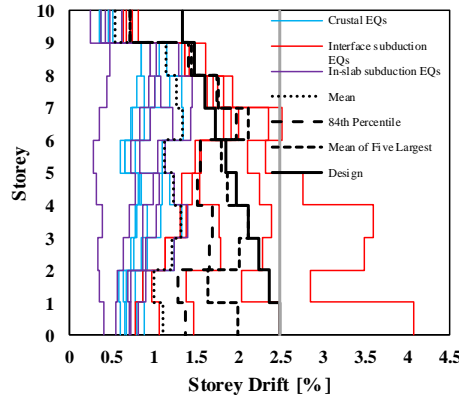


Figure 8. Maximum storey drifts for 10-storey FIEB designed with 2.5% target drift

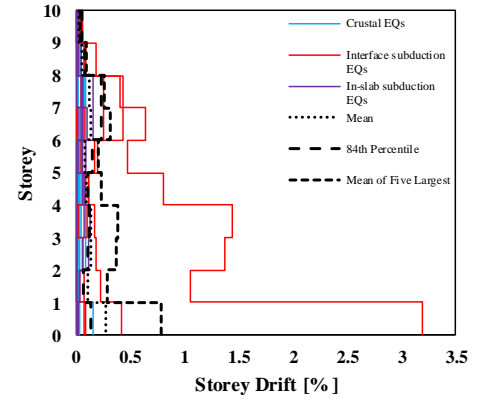


Figure 9. Residual storey drifts for 10-storey FIEB designed with 2.5% target drift

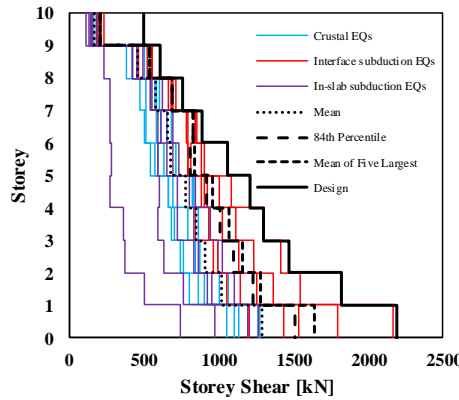


Figure 10. Maximum storey shears for 10-storey FIEB designed with 2.5% target drift

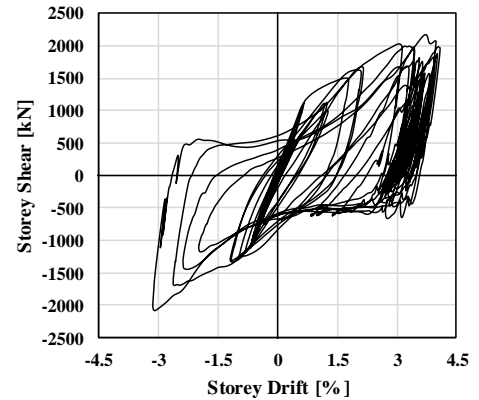


Figure 11. First storey shear vs. drift history plot for FIEB designed with 2.5% target subjected to the acceleration record that produced the largest demands (subduction)

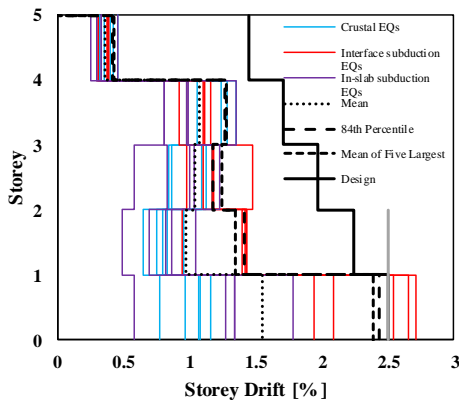


Figure 12. Maximum storey drifts for 5-storey FIEB designed with 2.5% target drift

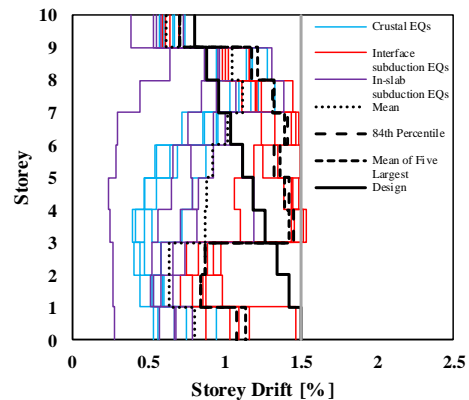


Figure 13. Maximum storey drifts for 10-storey FIEB designed with 1.5% target drift

In Figures 12 and 13, the maximum storey drifts obtained from the NLRHAs performed on the 5-storey FIEB designed for a target drift of 2.5 % and the 10-storey FIEB designed for a target drift of 1.5 % are presented, showing that the proposed design procedure could be, albeit preliminarily, deemed suitable for designing FIEBs of diverse heights and for different target drift ratios. In Table 1, the compared steel tonnages required for the buildings defined as Types LD- and MD- CBFs and as FIEBs is presented. The reduction in material required for the FIEB system in comparison with the Types LD- and MD- CBFs is mainly due to the lower capacity-based design forces that govern the design of the protected beams and columns.

Table 1. Compared steel weights for LD- and MD-CBFs and FIEBs.

Steel Tonnage [t] per braced frame	Braced Frame Type		
	LD-CBF	MD-CBF	FIEB
5 Storeys	19.1	15.0	12.0
10 Storeys	63.7	46.0	25.6

## CONCLUSIONS

It was shown in the preliminary review described herein that BIEs can function as an alternative to conventional CBBs. Their use overcomes some of the principal drawbacks of CBBs, most notably their susceptibility to low-cycle fatigue induced fracture and large inherent stiffness.

A preliminary design procedure based on the displacement-based design approach has been implemented as the conventional methodologies used for CBF design are inappropriate for the BIEs particular force-deformation behaviour. Designs carried out with this proposed procedure have yielded promising results. BIEs seem suitable to constitute SFRSs complying with the NBCC 2015 limiting drift ratios and capacity-based design philosophy in regions with high seismic hazard, while being economically advantageous. Further studies, however, are required to generalise these statements, including laboratory testing of full-scale BIE specimens constructed using North-American materials and fabrication techniques. Moreover, further research is needed regarding the equivalent damping ratios and design displacement vectors that are required in the method.

## ACKNOWLEDGMENTS

The first author wishes to thank Universidad de Costa Rica for financing the undertaking of his doctoral studies. The authors would like to thank the ADF Group Inc. and DPHV Structural Consultants for their generous technical and financial support, as well as the Natural Sciences and Engineering Research Council of Canada.

## REFERENCES

- [1] CSA (2014). *CSA S16-14: Design of steel structures*. Canadian Standards Association (CSA), Toronto, ON.
- [2] Tang, X., Goel, S. (1989). "Brace fractures and analysis of phase I structure." *ASCE Journal of Structural Engineering*, 115, 1960-1976.
- [3] Tremblay, R., Haddad, M., Martínez, G., Richard, J., Moffat, K. (2008). "Inelastic cyclic testing of large size steel bracing members." *Proc. 14<sup>th</sup> World Conference on Earthquake Engineering*, Beijing, China, Paper no. 05-05-0071.
- [4] Skalomenos, K., Inamasu, H., Shimada, H., Nakashima, M. (2017). "Development of a steel brace with intentional eccentricity and experimental validation". *ASCE Journal of Structural Engineering*, 143 (8).
- [5] McKenna, F., Fenves, G., Scott, M. (2004) *Open System for Earthquake Engineering Simulation*. Pacific Earthquake Engineering Center, University of California, Berkeley, California.
- [6] Priestley, M., Calvi, G., Kowalsky, M. (2007). *Displacement-based seismic design of structures*. IUSS Press, Pavia.
- [7] NRCC (2015). *National Building Code of Canada 2015, 14<sup>th</sup> ed.* National Research Council of Canada(NRCC), Ottawa, ON.
- [8] Wijesundara, K., Rajeev, P. (2012) "Direct Displacement-Based Design of steel concentric braced frames structures." *Australian Journal of Structural Engineering*, 13 (3), 243-257.
- [9] O'Reilly, G. Goggins, J., Mahin, S. (2012). "Performance-based design of a self-centering concentrically braced frame using the Direct Displacement-Based Design Procedure". *Proc. 15<sup>th</sup> World Conference on Earthquake Engineering*, Lisbon, Portugal, Paper no. 918.
- [10] Salawdeh, S., Goggins, J. (2016). "Performance-based design approach for multi-storey concentrically braced frames". *Steel and Composite Structures*, 20 (4), 749-776.
- [11] European Committee for Standardization – CEN (2004). *EN 1998-1:2004 Eurocode 8: Design of structures for earthquake resistance – Part 1: General rules, seismic action and rules for buildings*. CEN, Brussels, Belgium.
- [12] Tremblay, R., Atkinson, G., Bouaanani, N., Daneshvar, P., Léger, P., Koboevic, S. (2015). "Selection and scaling of ground motion time histories for seismic analysis using NBCC 2015". *Proc. 11<sup>th</sup> Canadian Conference on Earthquake Engineering*, Victoria, BC, Paper no. 99060.